Experimentation of a Multi-Threaded Distributed Telerobotic Framework

Mayez A. Al-Mouhamed[1], Mohammad Nazeeruddin[2], and Syed M.S. Islam[3]

Abstract—A multi-threaded distributed telerobotic system (MTDTS) was proposed. MTDTS consists of a client station (operator) and a server station (slave arm) interconnected by a computer network. MTDTS is evaluated using a set of tele-operated experiments which are (1) peg-in-hole insertion, (2) assembly of a small water pump, (3) operating drawers, (4) pouring of water, and (5) wire-wrapping. Direct teleoperation is evaluated using following schemes: (1) stereo vision, (2) vision and force feedback (FF), and (3) vision with active compliance. Space indexing and scalability tools are also used. Operator hand is logically mapped to a remote tool both in position and force. The operator feels the forces exerted on the tool as they were exerted on the hand. Mapping of operator hand motion and FF to a convenient tool point reduces operator mental load and task time due to highly-coordinated motion and cartesian FF mapping. With active compliance all tasks are done in the least task times and with the least contact forces. Stereo vision may alone be used but with large peak forces and extended task time. Force feedback has nearly equal task time as compared to active compliance but with a noticeable increase in contact forces. Force feedback and active compliance are critical tools for extending human eye-hand motion coordination and dexterity to remote work in hazardous, hostile, inaccessible, and small-scale environments.

Index Terms—Active compliance, assembly, force feedback, insertion, motion coordination, stereo vision, teleoperation.

I. INTRODUCTION

TELEROBOTICS aims at extending human natural eye-hand motion coordination over an arbitrary distance and an arbitrary scale. The objective is to replicate manipulative skills and dexterity to a remote work place. Human psychomotor skills have evolved over million of years. The design of effective man-machine interfacing and the transmission delays are two major limiting factors.

A 3D virtual reality model [1], [2] of the environment is used to develop model-based assistances and mixed control modes in repeatedly performing a sequence of short modelling, programming, and execution. A virtual arm is teleoperated, accessibility is checked, valid paths control the slave arm, and feedback from slave arm is used to controls the virtual arm. The system is used in unfastening 12 nuts of a tap cover, lifting up a cover using gantry crane, inspecting the tap, and lifting down the cover and fasten it again.

An event-driven virtual reality (VR) [3] is used to model the environment to ease the task of programming, planning,

(1) Department of Computer Engineering, College of Computer Science and Engineering (CCSE) King Fahd University of Petroleum and Minerals (KFUPM), Dhahran 31261, Saudi Arabia. mayez@ccse.kfupm.edu.sa

(2) Department of Systems Engineering, CCSE, KFUPM, Dhahran 31261, Saudi Arabia. nazeer@ccse.kfupm.edu.sa

(3) Department of Computer Engineering, CCSE, KFUPM, Dhahran 31261, Saudi Arabia. shams@ccse.kfupm.edu.sa

and teleoperating a remote robot. Once the VR assemblies are set up placed, the real links update their recorded trajectory. This approach is useful to resolve conflicts among multiple robots while reducing communication bandwidth.

In [4] a sensor-based motion-planning is proposed for teleoperation in deep space. Bilateral control of a graphic slave arm operating on a 3D graphic environment is used to select an approximate sequence of fine motions. The operator is provided with graphic animation using kinematics, dynamics, friction, and impact forces used in a closed loop control provides the operator the feeling of repulsive forces. A 3D collision prevention scheme is used. The sequence is sent to a slave arm supervised by a sensor-based motion-planning algorithm and applied to peg-in-hole assembly. Accurate graphic and physical models of slave arm and environment are needed.

Using a pre-planed insertion path, adaptive impedance control (AIC) [5] is used to reduce jamming forces by finding the desired position adaptively to follow the optimal path from the current position and environmental constraints. For peg-in-hole operations, the scheme may correct slight horizontal misalignment due to uncertainties. A two-level Teleoperation scheme [6] is proposed for the Wearable Energetically Autonomous Robot (WEAR). The masters emit lower-level commands using the natural intelligence of the operator. To make decisions for the management of the robot, AI-based commands blend higher level simple commands with system and existing environmental states.

Bilateral control is essential to replicate human performance at a remote site. Theoretical analysis of stability/performance for position error, Lawrence 4-channel, and 5-channel schemes for teleoperation [7] found that a compliant slave device provides some stability advantage over a built-in passive intrinsic stiffness. A direct bilateral teleoperation (DBT) with kinesthetic force feedback is very useful even with a round trip delay of 6 seconds [8]. Peg-in-hole insertion with 0.4 mm clearance and slope tracing are still feasible using a stable PD controller without the use of scattering theory to guarantee stability. A gain-switching control [9] proved to improve the teleoperation transparency when using constant controller gains in position-error-based teleoperation during slave free motion or when colliding with a stationary stiff environment.

An anthropomorphic space robot is evaluated using kinesthetic and stereo HMD [10]. The operator position is mapped to slave arm both is position and velocity. Evaluation of a drill task indicates less contact forces with equal task time when either visual or kinesthetic force is used with stereo vision. A mixed of direct and task oriented modes [11] are activated

using a set of visualization and manipulation tools with some force monitoring to improve safety and accuracy in micro/nano spaces. To avoid collision high-level motion commands are used due to electrostatic forces and possible sticking. For legged robots [12] the use force sensing is useful to measure the foot-ground force interaction as well as the ground-reaction forces and to compute the zero-moment point in real time while standing or executing a dynamically balanced gait.

In surgery, force sensing is indispensable for reliable perception of the stiffness of soft tissue [13] to discriminate tinier differences in telemanipulation with enhanced sensitivity than through direct manipulation. The use of force feedback during micro surgeries [14], [15] indicate that typical forces on the microsurgical instrument tips during the retinal surgery are less than 7.5 mN, which is below the threshold of the operators tactile sensitivity. Unless these contact forces are properly amplified, the surgeon will not be able to sense them. Thus, the surgeon may operate with little or no tactile feedback which increases the potential of tissue damage. To measure the contact forces a miniature force sensor [14] is used at the tip of a microsurgical instrument. A position-controlled motion is proposed with micrometer resolution for force-feedback of no less than 5 mN. The use of force-feedback in remote endoscopic surgery [16] proved to be beneficial. The slave manipulator accurately and quickly mimic the movement of the master arm at low speed; and the master arm satisfactorily reproduced the force. Force-feedback [17] is also effective in suturing rabbits neck artery (3mm in diameter) and leg artery (1mm in diameter).

A telerobotic framework is evaluated using direct teleoperation with following schemes: (1) stereo vision, (2) vision and force feedback, and (3) vision with active compliance. Indexing and scalability tools are used. The proposed system is used to carry out a set of experiments involving contact with the environment. Operator hand motion is mapped scheme to remote tool both in position and force. Strategy for task effective execution is presented for each experiment. Analysis of operator interaction with the environment, task time, and peak and average contact forces is presented. Comments on the global performance of each scheme is presented together with a comparison to other contributions.

The organization of this paper is as follows. In Section 2 the telerobotic system is presented. In Section 3 the description of experimental tasks is presented. In Section 4 the used tools and strategy for the experiments are presented. In Section 5 the experimental results are presented. In Section 6 some results are compared to other contributions. We conclude in Section 7.

II. TELEROBOTIC SYSTEM

Telerobotics allows extending eye-hand motion coordination through a computer network. Motion scalability establish a mapping from human scale to an arbitrary target teleoperation scale (micro, nano,etc.). Performance is measured by the extent to which telerobotics preserves human manipulative dexterity and by the fidelity in translating the physical laws from scale to another. Telerobotics is based on developing a multi-disciplinary research environment integrating motion, vision, and haptic senses to experience manipulative tasks, system interactions, man-machine interfacing, and computer aided teleoperation (CAT). For this a Telerobotic Client (TC) having a master arm station is interconnected through the Internet to a Telerobotic Server (TS) having a slave arm station. TC and TS implement the bilateral master-slave interconnection at the Cartesian coordinate level, motion coordination system, teleoperation tools, and streaming of video data (stereo vision) and force feedback.

A. Client-server telerobotic system

A schematic diagram of our telerobotic system is shown in Figure 1. The TS has three modules: (i) a 6 dof PUMA 560 slave arm module ($Server_{puma}$); (ii) a force sensor module ($Server_{force}$); (iii) a video module ($Server_{video}$). Similarly, the TC also has three modules: (i) a locally developed master arm ($Client_{master}$); (ii) a force display ($Client_{force}$); (iii) a video display ($Client_{video}$). The master arm is a light, 6 DOF, wire-based, anthropomorphic, arm that was designed and manufactured at King Fahd University of Petroleum and Minerals (KFUPM) currently being patented. The telerobotic system software is implemented such that all the TS and TC modules run simultaneously as concurrent, independent, programs (threads).

Streaming of real-time data through the network is carried out as a logical mapping from $Server_{video}$, $Server_{force}$, and $Client_{master}$ to $Client_{video-disp}$, $Client_{force-disp}$, and $Server_{slave}$, respectively. Each of the above modules has layered structure for information processing ranging from the physical sensor data level to the computation of a higher level information such as tool motion or tool force. In the following we shortly describe the function carried out by the above peer processes.

The $Client_{master}$ regularly samples the master arm, computes variation in operator hand position and orientation using forward arm kinematics, and transfers the above variations to $Server_{PUMA}$. Upon reception of above motion variation the $Server_{puma}$ updates the slave arm tool position with received data using forward and inverse arm kinematics and commands the slave motion accordingly.

The $Server_{force}$ regularly samples wrist force sensor, evaluates the force applied to the tool, and streams the computed force to $Client_{force-disp}$. The $Client_{force-disp}$ receives force data, computes the implied master arm motor torques using jacobian transformation, and displays the resulting torques on the master arm motors.

The $Server_{video}$ continuously grabs video images from left and right digital cameras and transfers them to $Client_{video-disp}$. The $Client_{video-disp}$ modules streams received video data on the left and right screens of a head-mounted display (HMD) to provide 3D visualization for the operator.

The TS and TC are implemented in a client-server architecture that reliably transfers stereo, force, and command data. Moreover, TS and TC use the distributed software approach so that modification of a module in one station does not
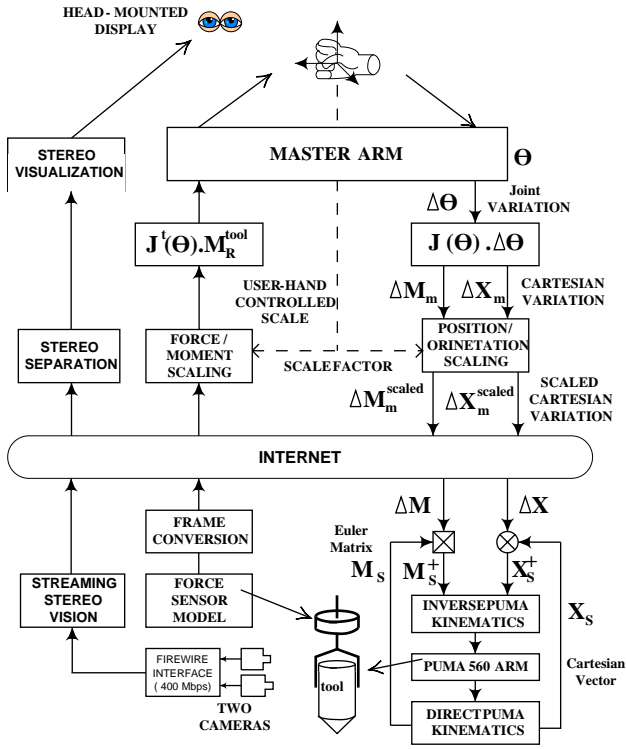
Fig. 1. Real-time transfer of motion command, force data, and live stereo video.

require software revision in the other station, i.e. the module functions are distributed in different software components. Specifically each module communicates with its counterpart using a standard inter-process communication system (MSF .NET remoting) which allows a module to to indirectly invoke (call) the functions of the other module without explicit network communication programming.

B. Force feedback and Active compliance

At the slave station, the PUMA 560 wrist force sensor is used to measure the effective force (F_w) and torque (C_w) exerting at the wrist. Using F_w and C_w, a geometric transformation allows computing the force vector (F_t) and torque vector (C_t) exerting on the slave arm tool. For direct teleoperation with reflected force feedback, both tool force vector F_t and torque vector C_t are streamed from the slave station (slave arm) to the client station (master arm). At the client station, received vector F_t and C_t are used to compute the master arm motor torque vectors $\Gamma_{mot} = J_{master}^t\{F_t, C_t\}$ which allows displaying (replicating) the F_t and C_t at the operator hand center, where J_{master}^t is essentially the master arm jacobian matrix computed for the current arm configuration. For teleoperation with active slave arm compliance, the force feedback is not streamed to the client station but locally used at the slave station to generate local force compliance. To obtain a spring effect on the slave tool, we use the above force and torques vectors to evaluate the elementary tool translation vector ΔT_t the elementary tool rotation matrix ΔM_t. Specifically, the above vectors are computed using the force $F_t = (f_x, f_y, f_z)^t = K_l \Delta T_t$ and torque $C_t =$

$(c_x, c_y, c_z)^t = K_r \Delta M_t$ vectors, where K_l and K_r are two empirical passive compliance matrices for linear and rotational motion of the tool, respectively. More details can be found at [18].

C. Network and system specification

In this section the specification and configuration of the network, software, and computers used are presented prior to addressing the analysis of experimental results of the telerobotic framework [19].

The client and server are run on two PCs having 2-GHz Intel P4 processors with 1GB DRAM and 512 KB cache memory. Each of client and server PCs is attached to a campus network by using a 100 Mbps NIC card. The server PC is interfaced to two Sony Handycam digital cameras using a 400 mbps FireWire PCI card. The client PC uses an NVIDIA display adaptor to interface with an SVGA resolution Cy-visor 3D Head-Mounted Display (HMD).

Both client and server PCs run under MS Window 2000. The vision server software uses MS Visual C++ with .NET framework 1.1, 2003. The PUMA server is implemented using MS Visual C# with the above .NET framework.

The connectivity between the client and server stations is defined as follows. Each packet travels across two L2/L3 switches using 100 Mbps input links, one L3 backbone switch that uses 1 Gbps link at input and output, and two L2/L3 switches using 1 Gbps links and two 100 Mbps hubs.

The network performance analysis and delay evaluation were carried on for the proposed telerobotic system. Brief results are reported here. Analysis of telerobotic delays through three campus routes was carried out while streaming of video, force, and commands. A sampling rate of 120 Hz is achieved for force feedback and 50 Hz for operator commands. Stereo video transfer operates at a rate of 17 fps. Total reference delays for force and stereo are 8 ms and 83 ms, respectively. Overall round-trip system delay between client and server is 183 ms (5.5 Hz) when slave arm is operated at 10 Hz. Delays introduced by the operator significantly vary from one operator to another. The above delay does not include the delays introduced by the operator such as the time spend on the apprehension of force feedback and stereo information and the corresponding reaction time. More details can be found in [20].

In the following Section, we present the experimentation details by considering the task description and specifications.

III. TASK DESCRIPTION AND SPECIFICATION

In this section we describe the experimental part of a multi-threaded distributed component framework for telerobotics. In the following sub-sections experiments are presented with their geometric and mechanical specifications.

A. Peg-in-hole insertion

The objective is to expose the proposed framework to an operation involving the following aspects: (1) teleoperation with kinesthetic force feedback display at the master arm or

(a) Peg-in-hole parameters and chamfer geometry

(b) Assembly part parameters and clearances.
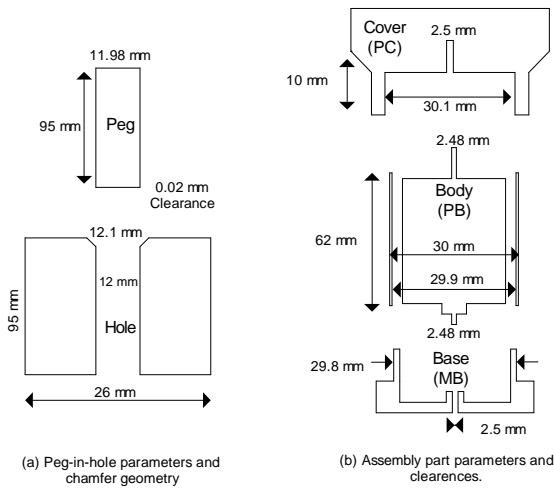
Fig. 2. Features and parameters of the peg-in-hole and pump components

(a) Drawer parameters

(b) Parameters of Wire-wrapping needles and tool

Fig. 3. Dimensioning parameters of drawers and wire-wrapping experiments

with active compliance at the slave station, (2) logical mapping of operator hand motion to a floating tool frame (TF) attached to a peg, (3) use of available computer-aided teleoperation (CAT) tools. Insertion deals with grasping of a peg, moving it to the top of hole, detecting contact with the hole, and inserting the peg in hole. The geometric dimensions, clearance, and chamfer geometry are shown on Figure 2-(a). For smooth insertion, the peg tip was rounded and the hole was chamfered. To avoid damaging the robot and sensors the hole was attached to a 1 kg base for which the sideways movements are permitted in response to a lateral force exceeding 8 N.

B. Assembly of a pump

This assembly requires a high-degree of eye-hand motion coordination with balanced dependence on both vision and force feedback. In the studied case the assembly operation requires one or two objectives to be met at the same time. The mechanical tolerance of the parts is relatively moderate as compared to that of the peg and the hole. These are shown on Figure 2-(b). A car water pump is used to carry out assembly and disassembly operations. The pump consists of three cylindrical parts: (1) a plastic cover (PC), (2) a metallic base (MB), and (3) a pump body (PB) which contains a motor to be assembled in the middle of the above two parts. The motor shaft axis appears on both top and bottom sides of PB. Initially MB is attached to a fixed platform for which the sideways movements are permitted in response to a lateral force exceeding 8 N. MB can be tilted by up to an angle of 10 degrees with respect to horizontal plan. The task is to grasp PB, move it to top side of fixed MB and carry out part mating of PB and MB. Then the above operations are repeated to assemble PC on the top on PB-MB compound.

C. Operating drawers

The task of operating drawers requires a high-degree of eye-hand motion coordination with moderate use of force feedback. The used drawer has a small vertical wing at its end to block its entire retrieval by only sliding it outward.
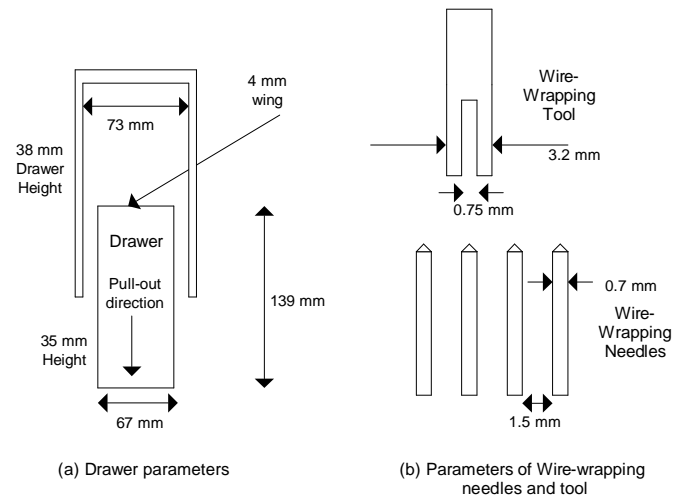
(a) Contact force/moment and tool frame location for coordinated teleoperation.

(b) Assembly parts (left), base-body sub-component (mid), and base-body-cover assembly (right).
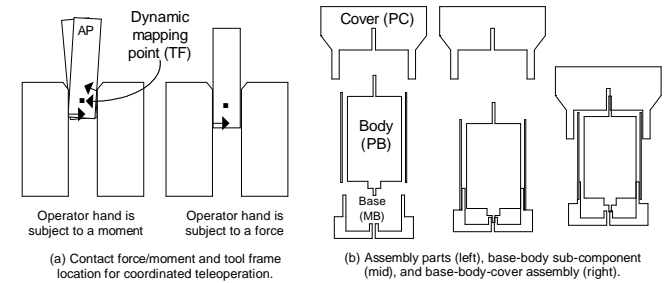
Fig. 4. Strategy used for peg-in-hole insertion and assembly of a water pump.

Once it reaches the blocking position at its end, the removal of the drawer requires (1) tilting it upward to free its bottom, and (2) sliding it downward to free its top. Figures 3-(a) shows the specification of the drawer used.

D. Pouring

The objective is to expose the proposed framework to the following aspects: (1) teleoperation with fine trajectory and time control, (2) extensive use of eye-hand motion coordination, (3) perception of 3D scene and scene depth, (4) evaluation of functional and ergonomic aspects of proposed CAT tools. This task deals with grasping of a small cup that contains colored water using the slave arm gripper, moving it to the neighborhood of an empty cup, and pouring the water in the target cup.

E. The wire-wrapping operations

The objective is to evaluate performance of proposed teleoperation system in a scaled-down slave arm space. The task is to insert the head of the wire-wrapping tool into a series of needles of a wire-wrapped electronic circuit. The operation must repeat from one needle to next in a row of 5. Figures 3-(b) shows the specification of the wire-wrapping gun and needles.

IV. EXPERIMENTAL METHODOLOGY

In this section each task will be analyzed with respect to tools used during its teleoperation, methodologies used to ease

Insertion using Force Feedback VFF:
(a) motion in direction of constraints, (b) avoid
constraint and zero force, and (c) searching to
nullify force in opposite direction.

Insertion using Active Compliance VAC:
(a) approaching hole and contact, (b)
insertion attempts, progress in depth,
and contact with hole bottom.
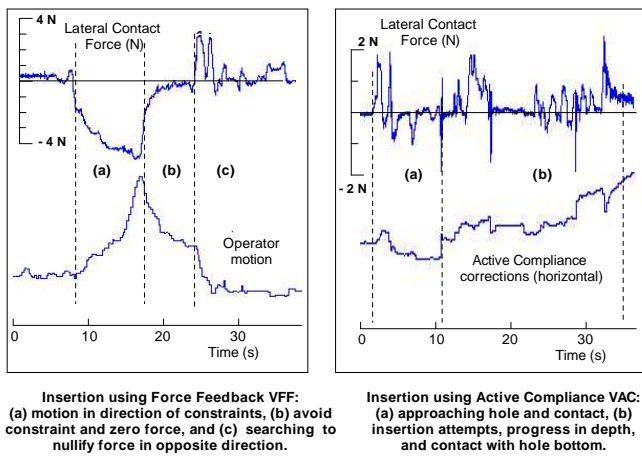
Fig. 5. Insertion using force feedback (a) and active compliance (b).

its achievement, and obtained results. This Section is organized as follows. We first present the specifications of the telerobotic system and its delays. Next, the task strategy, experimental analysis, and results of carrying out each of the tolerobotic tasks are presented. Video clips on these experiments can be found at [21].

A. Peg-in-hole insertion

The peg-in-hole insertion consists of searching an unconstrained motion path in a space constrained by the jamming F/M. The peg is held by the slave arm gripper. To start, the peg is held in the axial direction of the hole to the best of operator and the 3D vision system. The displayed 6D force feedback represents the forces exerted on the slave arm tool to which the peg is firmly attached. Here 3D vision perception provides coarse information while displayed force feedback is critical to search unconstrained motion directions based on correcting both peg-hole axial and rotational mismatches.

Using the operator-arm interface, a static mapping (S-1) is to link the operator hand to the arm-peg (AP) attachment point. At the server, this mapping also enables computing the external force and moment (F/M) in a frame of reference centered at AP. At the client, the computed external force is displayed at the operator hand using the master arm. Here the stereo vision is not very helpful in making fine translational or rotational motion corrections. Since the operator hand is logically mapped to the peg at point AP, a single F/M contact component corresponds to a subset of coupled F/M being sensed by the operator at AP which might defeat the operator action to nullify above F/M by simple hand motion. We found that it is difficult for a human to comprehend an F/M compound, applied to hand, as opposed to a single F/M component. Therefore setting the motion mapping should be guided by the need to uncouple contact F/M in an attempt to reduce the operator mental load and operation time. For this mapping S-1 was abandoned due to lack of efficiency.

Another mapping (S-2) consists of initially setting the mapping point at the edge of the peg and dynamically compute the new mapping

point by locating it in the middle of peg part that is already inserted in the hole as shown on Figure 4-(a). This can be evaluated using (1) the horizontal plan at the top of the hole which is taken as reference for zero depth and (2) current peg depth. This strategy aims at capturing the jamming F/Ms where they are exerted on the peg and display them on the operator hand to favor direct corrections of both peg-hole misalignment errors (moment) and translational errors (force). Hence the objective of this mapping is to logically map the operator hand at a point where it is: (1) effective to capture the mechanical constraints such as the jamming forces, and (2) easy to make necessary correction through motion mapping. Since the above point is dynamically re-mapped to the operator hand motion, thus, the operator rotational and translational corrections are likely to reduce the above constraints due to the one-to-one mapping of the jamming constraints and the corrective motion done by the operator. The scalability function is used here to scale-down the operator motion in all directions to allow fine (1) motion correction in the horizontal plan, and (2) position control of the force exerted by the peg on the hole. Visual monitoring is also used to appreciate the progress in the insertion.

Figures 5-(a) and (b) show performance of peg-in-hole insertion using teleoperation with stereo vision and (1) force feedback (VFF), or (2) active compliance (VAC). The upper and lower plots correspond to displayed force feedback and operator motion command, respectively. These interactions are exchanged through the network. In step (a) of VFF, the operator searches an unconstrained motion path in a space constrained by a contact force (-4 N), e.g. a wall effect. In step (b), operator changes direction and reduces lateral contact force which allows the peg to go deeper in the hole. In step (c), a different contact force appears and the same cycle is repeated until completion of insertion.

The third approach (S-3) consists of a supervisory corrective motion done by the local force regulation and the remote slave arm. This solution is similar to the second mapping in terms of measurement of mechanical constraints at the above floating TF but instead of forwarding contact F/M to the operator, active compliance controller is activated at the slave station (shorter loop) which leads to superimpose locally computed peg motion corrections (rotational and axial corrections) to motion instructed by the operator. In this case the operator may limit his control of the peg to vertical direction with the corresponding force feedback. The space scalability function is used here to scale-down the operator motion in the horizontal plan (10:1) with a unit scale in the insertion direction which allows the operator to control the vertical force the peg is exerting on the hole.

In Figure 5-(b) an active compliance control is set at the server. The upper and lower plots correspond to displayed contact force measured at the server and the motion correction made by active compliance controller, respectively. These interactions are local to the slave station. The operator applies a downward force (step (a)) while active compliance control searches a horizontal position and orientation (step (b)) that reduces contact F/M components. Due to proper mapping, F/M components are likely to be uncoupled from each other and

Assembly using force feedback VFF:
(a) approaching pump-base and contact,
(b) part mating of body and base, and (c)
removal of body.

Assembly using active compliance VAC:
(a) corrections made by AC while operator push
downward for part mating, (b) operator removes
body and reaction of AC.
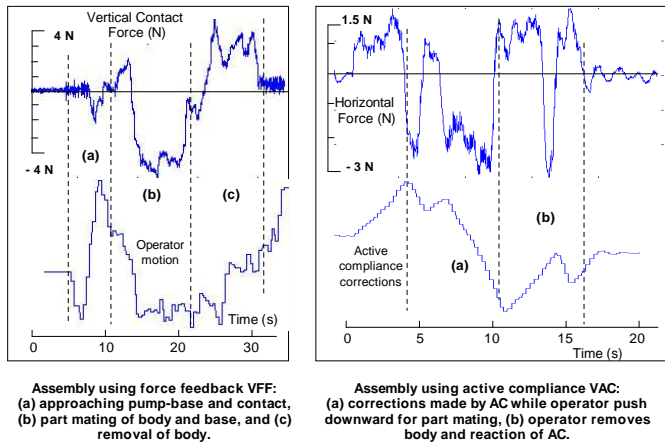
Fig. 6.   Assembly using force feedback (a) and active compliance (b).

corrected independently from each other. This results in the lowest exposure to contact forces.

B. Assembly of a water pump

The assembly plan is as follows. PB is grasped and moved to the vicinity of MB. Operator carries out axis alignment to the best of the available 3D depth perception. The steps are shown on Figure 4-(b). Part mating requires meeting two constraints which are (1) force contact of the motor shaft axis and insertion in the middle hole of MB, and (2) part mating of both lateral cylinders of PB and MB while maintaining axes alignment. The above constraints must be met in a sequential order starting with the best possible configuration that can be achieved using 3D stereo vision and later combining both force feedback and visual information. Similar operation is carried out for assembling PC on the top on PB-MB compound.

The assembly strategy consists of using a balanced mixing of visual and force feedback in addition to space scalability to maintain some geometric directions and keep correcting other references. Specifically the visual feedback is used to establish a proper geometric setting in the pre-positioning phase. The operator space mapping in the horizontal plan is scaled down, for example by a factor of 10:1, to maintain the part position-ing and to limit potential motion in the horizontal plan. The vertical axis is left with unit scale under operator control. This approach allows preserving axis alignment (first constraint) of the parts during the part mating operation (second constraint). It allows the operator exerting fine force control in pushing one part into another while monitoring the results. In the case of large positioning errors or axis misalignment during the part mating operation, the tool is lightly lifted up (failure) and the space scalability is increased (for example to 3:1). Correction of part position and orientation are made before attempting again the part mating phase. Force feedback is critical in carrying out the part mating in which the part is subject to a soft down-ward push under careful visual monitoring using zoomed stereo vision for the early detection of potential mismatch. In summary, successful part mating is based on a combination of fine force feedback and 3D depth perception in addition button-controlled tools like indexing and scalability.

(a) Drawer removal, initial setting (top), and
coordinated motion removal (bottom).

(b) Operator intuitive pouring (left), and operator
coordinated pouring (right).
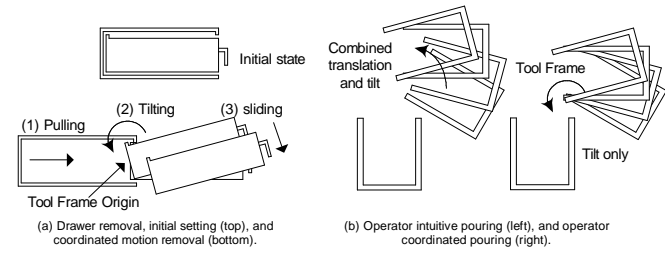
Fig. 7.   Strategy used for operating a drawer and pouring water

Figures 6-(a) and (b) show performance of assembly tasks schemes VFF and VAC, respectively. Under VFF scheme, in step (a) PB is moved by the operator to MB where a contact force is detected. Pre-positioning and part mating are performed in step (b). Notice the force feedback (wall effect) displayed on the operator. In step (c) PB is extracted from the assembly with a release force feedback and return to zero force once in free air. The fluctuations in force are caused by the friction.

In Figure 6-(b) the sensed contact force is used by the active compliance to carry out corrections of position and orientation of PB while the operator attempts the part mating. Part mating is performed in step (a). Notice the resulting force feedback when the part hits the bottom of MB. In step (b) PB is extracted from the assembly with an additional release force feedback and return to zero force once in free air. The contact forces involved have less magnitude and time than those of the VFF scheme.

C. Operating drawers

The drawer is pulled up until its bottom wing reaches the blocking point. During the above operation motion scalability can be used to scale down the operator motion in all directions except the pulling direction to maintain directional motion. The blocking end is detected using both visual and force feedback.

To ease the operator task TF must be located at end of the drawer so that the needed tilt operation can be made using a rotation about the horizontal axis of TF. Figure 7-(a) shows the initial closed drawer (up) and the steps for its opening and entire removal (down). For this, the GUI, AR tools, and master arm are used to point to the new TF origin O_{TF}. This allows relocating TF. Now the operator hand motion maps logically to TF and the contact F/Ms are now computed with respect to TF before being forwarded to the operator or locally used in the slave active compliance loop. This provides one of the best possible logical mapping from the operator hand to manipulated object so that the needed action is projected on one single axis at the new location of TF. In other words, the operator feels the contact between the wings with the environment as if the drawer is held by the operator. By tilting the hand in the upward direction the front side of drawer is tilted up which frees the drawer bottom that can now be shifted downward before becoming entirely free. During the above operations the displayed contact forces are very helpful in detecting potential contacts that may result from errors in

the location of TF and implied operator motion.

D. Pouring

The pouring operation consists of (1) grasping, (2) traveling, and (3) pouring. Grasping requires the slave arm to move down to a pre-apprehension configuration prior to grasping of a cup (FC) filled with colored water. This is done while continuously trying to center the jaw to middle of FC at its mid height to avoid potential collision. During grasping the indexing function is frequently used to maintain the master arm within a small operator dexterity area whenever the motion requires moving along a path consisting of a long translation or rotation. Traveling requires lifting FC and moving towards the target cup (TC) while maintaining the slave gripper in a horizontal plan and progressive setting up of FC orientation when approaching TC. Pouring requires setting up a proper pre-pouring configuration in the vicinity of TC. Now FC must be tilted while keeping its top above TC. This normally consists of a rotation and a translation as shown in the left part of Figure 7-(b). To reduce the workload on the operator it is more interesting to relocate the mapping function of the slave tool at one of the top lateral point of TC which becomes the origin of the new TF. In this case tilting the operator hand leads to directly tilting the new TF about one axis of above frame as shown in the right part of Figure 7-(b). We note that placing TF origin (and orientation) at the above critical point contributed in reducing the task time by about 40% as compared to default setting of TF at gripping point. In addition, it produces a predictable trajectory while being an ergonomic teleoperation tool.

E. The wire-wrapping operations

The GUI is used to set up (1) scale level of force feedback, and (3) the camera zooming level. The space scaling is directly controlled by the operator index. The converging setting consists of scaling the operator motion by a factor of 30:1, the force feedback by a factor of 1:10, and stereo camera zooming by a factor of 1:40. The operator moves the wire-wrapping tool (WWT) while aligning its axis with the circuit needle using 3D vision and carries out the insertion. The operator needs to feel the vertical force component to avoid damaging the needle during contact because actually only a small central hole in WWT must fit the needle as shown on Figure 3-(b). In this case the operator carries out corrections of axis mis-alignment, and (2) insert WWT head in the needle. The distance between two needles is about 1.5 mm. The above task was successful in making five successive insertions in a line in 30 seconds. The operator adaptation to teleoperation to small scale appeared to be smooth and simple. Multiple zooming views is useful to avoid changing the zooming level whenever axis alignment needs correction.

V. RESULTS AND DISCUSSION

In this section we present the global results of using the proposed telerobotic system in performing the above teleoperation tasks, the used CAT tools, and recommendations on how to improve the man-machine interfacing in the telerobotic system.
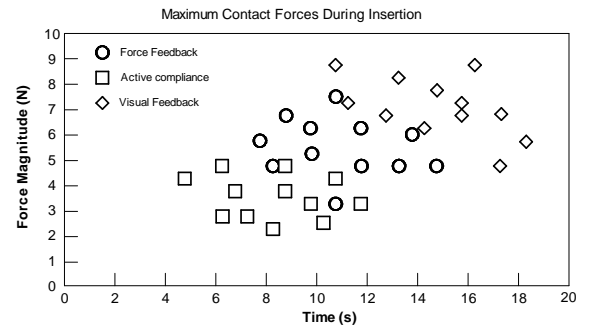
Fig. 8. Maximum insertion forces with respective task times
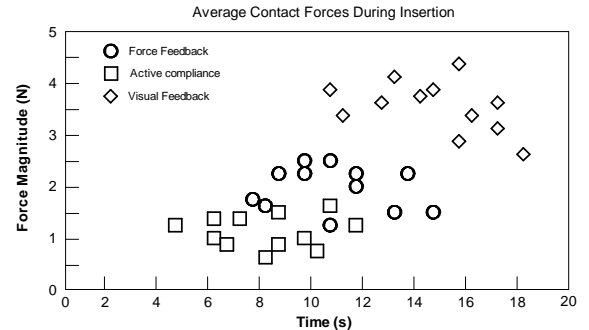
Fig. 9. Average insertion forces with respective task times

A. Analysis of teleoperation tasks

In this section we present the results of using the proposed telerobotic system in performing peg-in-hole insertion and assembly operation. These tasks are selected because they require effective interaction between the operator and the remote task involving fine motion, force feedback, and stereo vision. The results are limited to the period of interactions with the environment such as the insertion phase in peg-in-hole operation and part mating phase in the assembly operation. Both phases follow the contact detection phase. We study the following teleoperation schemes in which the operator has control of a 6 DOF master arm and provided with (1) only 3D visual feedback (V), (2) 6 DOF kinesthetic force feedback with 3D visual feedback VFF, and (3) visual feedback with active compliance VAC operating at the slave site.

Each of the insertion and part mating phases was carried out by 12 students aged between 18 and 24. The designer explained to them the various aspect of the telerobotic system for 2 hours. The objective function is to carry out the above two tasks in the least possible time while minimizing contact forces to reduce potential damage and improve operation effectiveness. The objective function was carefully explained and discussed to the students. Each student was allowed to experience the insertion and assembly tasks at least 10 times before recording the data. Thus the initial learning period for each operator is between one to two hours.

Each carried out successively schemes V, VFF, and VAC. Each scheme was carried out 12 times in total for each of the above two phases. The collected data refers to maximum and average F/M magnitudes as well as the corresponding completion time of a given operation for a given operator.
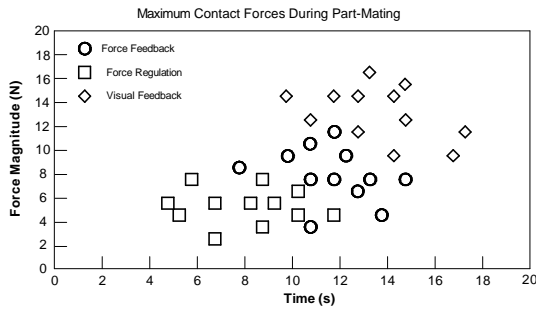
Fig. 10.   Maximum assembly forces with respective task times
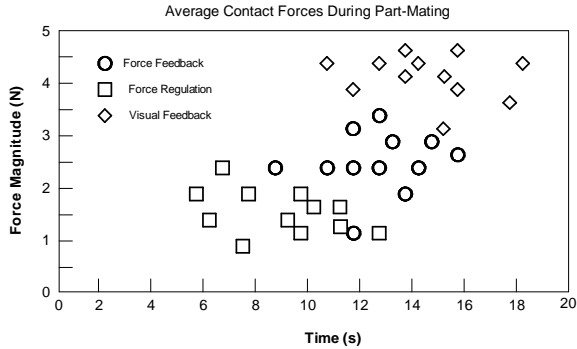
Fig. 11.   Average assembly forces with respective task times

Comparison of force and task time in insertion and assembly

	Force Magnitude		Task Time
Operation(ratio)	Maximum	Average	duration
Insertion (V/VAC)	1.93	3.85	1.76
Insertion (VFF/VAC)	1.45	1.89	1.33
Assembly (V/VAC)	2.33	2.74	1.55
Assembly (FF/VAC)	1.27	1.63	1.36

TABLE I

PEAK FORCE AND TASK DURATION FOR V AND VFF VS. VAC

Combined results for all operators are presented. In total we have 72 plots for two phases. The F/M vectors are all computed at the origin of reference TF and sampled at 50 Hz on slave arm station. Both force and moment components are similar in terms of concluding remarks.

Figures 8 and 9 show the maximum and average force exerted during peg-in-hole insertion with respective operation times. The operators were satisfied with the quality of stereo vision provided during the experiments. Scheme V allows completion of the insertion but with the largest contact forces and completion times as compared to VFF and VAC. Occasionally V scheme may produce less contact forces and possibly less duration than the other two schemes. Stereo vision is one critical operator augmentation in telerobotics. However, the use of only visual feedback for any operator indicates that another critical feedback is missing as both peak and average forces dominate as compared to the other schemes. The average force indicated some dependence on the operator speed and overall performance for a given operator. The ranking of any given operator performance is mainly the same in each scheme.

Figures 10 and 11 show the maximum and average force exerted during assembly of the pump with respective operation times. Similar to the insertion case, the VAC scheme outperforms the V and VFF but with less deviations both in maximum and average contact force. Table I shows the ratio of maximum and average force and task time of schemes V and VFF over scheme VAC for both insertion and assembly tasks. For the insertion, teleoperation with active compliance VAC allowed carrying out the tasks with the least task times and contact force. For the insertion, scheme V allows completion

of the insertion but with significant increase in contact forces and task time as compared to VAC. Teleoperation with VFF slightly increases task time but with a noticeable increase in contact forces as compared to VAC. VFF produces the largest variation in time from one operator to another. This shows that active compliance loop at the server station is better prepared to correct contact forces than the remote human. This shows the efficiency of supervisory approach and its local active compliance that continuously searches to nullify the external F/M by correcting tool position and orientation at current TF. Occasionally VAC gets higher times due to temporary blocking caused by excessive vertical force commanded by the operator.

For the assembly tasks, teleoperation with VAC is still ranked first but with less advantages as compared to the case of the insertion. The reason is probably due to operator ability to combine force feedback with 3D perception in the critical phases of the part mating.

In both insertion and assembly, VAC contributed in reducing peak and average contact forces as compared to both V and VFF schemes especially in the case of the insertion. VAC equally reduced task time for each of the FF and V schemes in both of insertion and assembly tasks.

Telerobotics needs advanced supervisory tools that embed complex force and position control with dynamic motion/force mapping. Effective man-machine interfacing is needed to integrate the above tools in a simple and natural way at the operator index and stereo space. The stereo space visible to the operator and its AR capabilities need to support the above integration. The connectivity between master and slave arms can be temporarily switched off and master arm used as a 3D pointer. A variety of active compliance (AC) scenarios can be associated graphical features in the operator stereo space. These can be selected and grouped in AC compounds (CACs) as task-oriented and operator favored tools. To activate a specific CAC at the task point of interest, the operator can point to a given CAC in stereo space, drag it, change its orientation, drop it at a desired tool point, and control its activation. This allows composing optimized AC mechanisms and efficiently activating them at the right location and orientation with respect current task.

VI. COMPARISON TO OTHERS

In virtual reality based teleoperation [1], [2], [3], [11] the operator plans an operation using a model, the plan controls a slave arm, and slave arm transmits back parametric feedback. The primary issue is operation safety. Mainly off-line approaches are used and teleoperation is carried out on a static environment with no dynamic interaction reported. However, in [4] graphic animation of robot kinematics, dynamics, friction, and impact forces used in a closed loop control provides the operator the feeling of repulsive forces which allowed to carry out peg-in-hole insertion. The proposed telerobotic framework provides direct-oriented teleoperation with CAT tools augmented with some supervisory control schemes to improve teleoperation effectiveness in real interactions with the environment.

We concur with [8] on the importance of kinesthetic force feedback in assembly operations. We extended direct teleoperation by using compliance control that makes the slave arm continuously searching to nullify F/M sensed on the current tool while the whole arm is being driven by the operator to take advantage of the above mechanism in current task. In comparison to [5] our proposed VFF and VAC schemes have similar effects in modifying task trajectory. The active compliance controller continuously searches corrections in tool position and orientation that reduce tool external F/M. Operator sets task-oriented compliance and leads the arm under compliance equilibrium to work location. Proposed VAC reduced peak contact forces and task time as compared to kinesthetic force feedback with vision in insertion and assembly tasks. VAC may also be useful as a task locality mechanism to ensure task continuity in delayed teleoperation. We use a constant controller gains in position-error-based for which the gain-switching technique proposed in [9] may improve sensitivity and transparency especially in the case of contact with rigid, elastic, or tissue objects.

The wrench mapping of [10] is comparable to proposed tool motion and force mapping. However, our dynamic mapping scheme showed to be useful tool for many tasks where the point of interest is function of task state. Proposed mapping makes the operator logically mapped, in position and force, to remote object. In addition we proposed indexing and scale tools and a tool-oriented dynamic motion mapping in position and force to carry out coordinated motion as a strategy to reduce operator cognitive load. This enables force reflection from current tool to the operator which increases the feeling of telepresence and enables teleoperation tasks to be completed more easily and with lower contact forces. The successful accomplishment of the above experiments is fundamentally due to the proposed dynamic mapping scheme which is estimated to be the most critical CAT tool in proposed telerobotics.

VII. CONCLUSION

A set of assembly tasks has been used to evaluate a client-server telerobotic system which transfers motion, force feedback, and stereo vision over a network. The tasks are (1) peg-in-hole insertion, (2) assembly of a pump, (3) operating drawers, (4) pouring of water, and (5) wire-wrapping. The operator has been provided with (1) stereo vision V, (2) vision and force feedback VFF, and (3) vision and active compliance VAC. Active compliance is has been used as assistance to direct teleoperation in addition to indexing and scalability tools. A dynamic mapping of operator hand motion and force to a task-oriented tool point has been used to reduce operator cognitive load and task time. Scheme V allowed to complete the above tasks but resulted in the largest contact forces and task times as compared to VFF and VAC. In contact centric tasks, like insertion, VAC noticeably outperforms V and VFF and provides task quality control. In multi-objective tasks, like assembly, VAC and VFF are closer in peak and average force as well as in task times. However, VFF has variable delivery as it depends more on operator skills. Button-controlled indexing and scalability proved to be the most frequently used tools. Scalability was useful to operate in a 30:1 scaled down space as well as a linear dimension blocking tool. Force feedback and active compliance are critical tools for extending human eye-hand motion coordination and dexterity to remote work in hazardous, hostile, un-accessible, and small-scale environments. To augment teleoperation a master arm-driven graphical tool is proposed for composing compliance mechanisms that can be dragged, attached to a tool point, and activated to ease man-machine interfacing.

REFERENCES

[1] E. Even, P. Gravez, E. Maillard, and E. Fournier. Acquisition and exploitation of a 3D environment model for computer aided tatleloperation. *Proc. of the 1999 IEEE Inter. Workshop on Robot and Human Integration*, pages 261–266, Sep. 1999.

[2] E. Even, E. Fournier, and R. Gelin. Using structural knowledge for interactive 3D modeling of piping environments. *Proc. of IEEE Inter. Conf. on Robotics and Automation*, pages 2013–2018, Apr. 2000.

[3] Bailin Cao, G.I. Dodds, and G.W. Irwin. An event driven virtual reality system for planning and control of multiple robots. *Proc. IEEE/RSJ Int. Conf. on Intelligent Robots and Systems, 1999. IROS '99*, 2:1161–1166, Oct. 1999.

[4] N. Funabiki, K. Morishige, and H. Noborio. Sensor-based motion-planning of a manipulator to overcome large transmission delays in teleoperation. *Proc. IEEE Int. Conf. on Systems, Man, and Cybernetics, 1999. IEEE SMC '99*, 5:1117–1122, Oct. 1999.

[5] Sukhan Lee, Ming-Feng Jean, Jong-Oh Park, and Chong-Won Lee. Reference adaptive impedance control: a new paradigm for event-based robotic and telerobotic control. *IEEE/RSJ International Conference on Intelligent Robots and Systems, 1998*, 2:1302 – 1307, Oct. 1998.

[6] S.C. Jacobsen, M. Olivier, F.M. Smith, D.F. Knutti, R.T. Johnson, G.E. Colvin, and W.B. Scroggin. Research robots for applications in artificial intelligence, teleoperation and entertainment. *The International Journal of Robotics Research*, 23(4-5):319–330, 2004.

[7] Goran A. V. Christiansson and Frans C. T. van der Helm. The Low-Stiffness Teleoperator Slave – a Trade-off between Stability and Performance. *The International Journal of Robotics Research*, 26(3):287–299, 2007.

[8] T. Imaida, Y. Yokokohji, T. Doi, M. Oda, and T. Yoshikwa. Ground-space bilateral teleoperation experiment using ETS-VII robot arm with direct kinesthetic coupling. *Proc. of the IEEE Int. Conf. on Robotics and Automation,ICRA 2001*, 1:1031 – 1038, June 2001.

[9] Liya Ni and David W. L. Wang. A Gain-Switching Control Scheme for Position-Error-Based Bilateral Teleoperation: Contact Stability Analysis and Controller Design. *The International Journal of Robotics Research*, 23(3):255–274, 2004.

[10] L.E.P. Williams, R.B. Loftin, H.A. Aldridge, E.L. Leiss, and W.J. Bluethmann. Kinesthetic and visual force display for telerobotics. *IEEE Inter. Conf. on Robotics and Automation, ICRA '02*, 2:1249–1254, 2002.

[11] A. Codourey, M. Rodriguez, and I. Pappas. A task-oriented teleoperation system for assembly in the microworld. *Proc. 8th International Conference on Advanced Robotics, 1997. ICAR '97*, pages 235–240, July 1997.

[12] Hector Montes, Samir Nabulsi, and Manuel A. Armada. Reliable, built-in, high-accuracy force sensing for legged robots. *The International Journal of Robotics Research*, 25(9):931–950, 2006.

[13] G. De Gersem, H. Van Brussel, and F. Tendick. Reliable and enhanced stiffness perception in soft-tissue telemanipulation. *The International Journal of Robotics Research*, 24(10):805–822, 2005.

[14] P.J. Berkelman, L.L. Whitcomb, R.H. Taylor, and P. Jensen. A miniature microsurgical instrument tip force sensor for enhanced force feedback during robot-assisted manipulation. *IEEE Trans. on Robotics and Automation*, 19:5:917–921, Oct. 2003.

[15] J. Arata et al. Development of a dexterous minimally-invasive surgical system with augmented force feedback capability. *2005 IEEE/RSJ Int. Conf. IROS*, pages 3207–3212, 2005.

[16] A. Matsui, K. Mabuchi, T. Suzuki, A. Namiki, M. Ishikawa, H. Fujioka, and H. Ishigaki. Development of a remotely-operated master-slave manipulation system with a force-feedback function for use in endoscopic surgery. *IEEE Inter. Conf. on Eng. in Medicine and Biology*, 2:1260 – 1263, July 2000.

[17] S. Wang et al. A robotic system with force feedback for micro-surgery. *Proc. 2005 IEEE Int. Conf. on Robotics and Automation*, pages 199–204, 2005.

[18] M. Al-Mouhamed, M. Nazeeruddin, and N. Merah. Design and analysis of force feedback in telerobotics. *AUS Inter. Symp. on Mechatronics*, April 2006.

[19] M. Al-Mouhamed, O. Toker, and A. Iqbal. A multi-threaded distributed telerobotic framework. *IEEE Trans. on Mechatronics*, 11(5):558–566, October 2006.

[20] M. Al-Mouhamed, O. Toker, and A. Iqbal. Performance evaluation of a multi-threaded distributed telerobotic framework. *Submitted for publication*, December 2005.

[21] Telerobotics video clips. *http://www.ccse.kfupm.edu.sa/researchgroups/robotics3*.